Transactions of the Materials Research Society of Japan 33[1] 99-102 (2008)

Preparation and Characterization of Micro-patterned Hybrid Bilayer Membrane

Yasuhiro Nishimura, Takaaki Manaka and Mitsumasa Iwamoto*

Department of Physical Electronics, Tokyo Institute of Technology, 2-12-1 O-okayama, Meguro-ku, Tokyo 152-8552

Tel/Fax: 81-3-5734-2562/2191, e-mail: iwamoto.m.ac@m.titech.ac.jp

Bio-mimetic membrane, hybrid bilayer membrane (HBM), was prepared on solid substrate using Self-Assemly and Vesicle Fusion (VF) methods. The HBM films were composed of self-assembled monolayer (SAM) of alkanthiol and phosphatidylcholine. Micro-patterned composite membranes of lipids were made on solid substrate with micro-patterned SAM by a micro-contact printing (μCP) method. AFM and Kelvin probe force microscopy (KFM) observation was conducted under height and phase modes, and surface potential, respectively. The height imaging showed that the flat surface was formed by the μCP method. Furthermore, the phase imaging and surface potential imaging revealed the micro-pattern formation. These results show that an artificial bilayer was successfully prepared on the surface without SAM, and lipid monolayer on the surface with SAM. These results were supported by the cyclic-voltammetry (CV) and surface potential.

Key words: lipid membrane, micro-contact printing (μCP), AFM, surface potential, dipole moment

1. INTRODUCTION

Since Singer and Nicolson proposed a famous fluid mosaic model of bio-membranes [1], many experimental and theoretical studies have been conducted to clarify the relationship between the function and structure of biomembranes. The preparation of mimic biomembrane systems is continuous study subject because one can get interesting function, e.g., self-healing effect [2], which is not be obtained by the use of ordinary organic molecular materials.

In our previous study [3], [4], we prepared two types bio-mimetic membrane on solid substrate. One was hybrid bilayer membrane (HBM) using self-assemly method and Vesicle Fusion (VF) method [5]-[8], where the first layer was self-assembled monolayer (SAM) and the second layer was phospholipids (Figure 1a). The other was micro-patterned HBM (p-HBM) using micro-contact printing (μCP) [9], [10], which was lipid membranes successfully prepared on the substrate coated with micro-patterned SAM (p-SAM) with a line and space structure (Fig. 1b). Afterwards, these biomembranes were characterized by cyclic voltammometry (CV) and AFM.

In our present study, after fabricating these p-HBM, we examined the physical and electrical properties of the prepared sample by using the surface potential and CV measurements.

Surface potential of prepared samples was measured by Kelvin probe family (Kelvin probe measurement: KPM and Kelvin probe force microscopy: KFM). Paying attention to the difference in the physical properties between single lipid layers and bi-layers, AFM and KFM observation were conducted under height and phase modes, and surface potential, respectively. The height mode AFM image revealed that the surface of prepared system was nearly flat over the entire region with a thickness of 5 nm, corresponding to the thickness of bilayer. On the other hand, the phase mode AFM and KFM images clearly distinguished between the single-layer region and bilayer region. The CV measurement showed that the deposited lipid layers on the surface of SAM and p-SAM blocks the redox-reaction electrochemically to some extent.

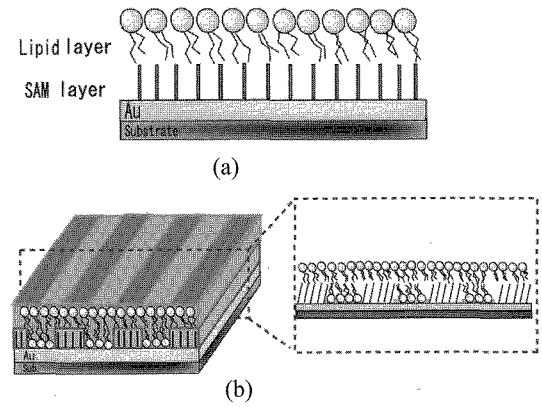

Figure 1 Schematic illustration of HBM (a) and p-HBM (b) on gold substrate.

2. Experiments

2.1 Materials.

1,2-Dipalmitoyl-sn-glecero-3-phosphocholine (DPPC) was purchased from Sigma Aldrich Japan (Tokyo, Japan). 1-Hexadecanthiol (HXDT) was purchased from Wako Pure Chemicals (Tokyo, Japan), and poly (dimethylsiloxane) (PDMS, Sylgard 184) was obtained from Dow Corning.

2.2 Preparation of substrates and Micro-contact Printing method

A 100-nm thickness Au-layer was evaporated onto glass substrates coated with a 20-nm thickness Cr adhesion layer. After cleaning the surface of the Au-layer with UV-ozone treatment, the SAM was deposited by immersing the substrate into a 2 mM ethanol solution of HXDT for 24 h at room temperature. Subsequently, the substrate was rinsed with ethanol solution several times.

On the other hand, p-SAM of HXDT was deposited using a PDMS stamp with a μCP method [9], [10]. A 2 mM ethanol solution containing HXDT was used as "ink" in the preparation. After the HXDT solution was applied to the PDMS stamp, this stamp was dried in air for 30 min, and then contacted with the prepared cleaned gold substrate in pure water for 10 sec. After the Au-layer substrate was taken out from pure water, the stamp was removed from the gold substrate. Finally the resulting substrate was dried in a stream of N_2.

2.3 Preparation of vesicle solution

Lipid layer was deposited by Vesicle Fusion method (VF)[5]-[8]. The preparation of VF solution was as follows: Once the lipids were thoroughly dissolved by 15 mg-lipid/ml in chloroform, the solvent was removed to yield a lipid film by using a dry N_2 gas flow. The resulting lipid film was placed in a vacuum desiccator overnight to remove residual chloroform. Hydration of the dry lipid film was accomplished by adding a buffer solution containing 150 mM-NaCl, 2 mM-$CaCl_2$ and 10 mM-HEPES (pH 7.0), and mixing by shaking. Afterwards, multilammelar vesicles were prepared.

The buffer solution temperature was set 50 ℃, above the gel-liquid crystal transition temperature (Tc) for DPPC (Tc: 41 ℃). The multilammelar vesicles were converted to small unilamelar vesicle by extruding the sample through polycarbonate membrane. Three filtration steps were performed using filters with pore sizes of 0.8, 0.4 and 0.2 μm sequentially, and finally the population of vesicles with a diameter below 0.2 μm was obtained.

Finally, for preparation of HBM or p-HBM, the SAM or p-SAM was immersed into the vesicle solution for 3 h at room temperature. Both of the samples were rinsed with buffer solution.

2.4 AFM observation, and Kelvin probe family measurements

AFM (NanoScope IIIa, Digital Instruments. Co. Ltd.,) was used for the observation of the surface morphology in air. Height and phase modes were selected for the AFM observation. By mapping the phase of the cantilever oscillation during the tapping-mode scan, phase imaging was recorded. Note that the phase imaging reveals variations in composition, adhesion, friction, visco-elasticity, and numerous other physical properties. Hence the phase mode enables us to image the difference in the physical property in the regions between deposited monolayer and bilayers.

The KFM (Nano Scope IIIa, Digital Instruments. Co. Ltd.,) and KPM (Trek) were used for the micro- and macro-area surface potential measurements of p-SAM, HBM and p-HBM in air, respectively. The KFM can visualize surface morphology and surface potential at the same time, and the electrostatic property of lipid monolayer and bilayer regions in p-HBM is evaluated.

2.5 CV measurement

To examine electrochemically the insulation and dielectric properties of the SAM, p-SAM, HBM and p-HBM, the CV measurements were carried out with an OMNI90 potentiostat (Cypress System) using a solution of 1 M-KCl with 1 mM-$K_3Fe(CN)_6$. The electrochemical cell used in this CV measurement was a three-electrode system with a Ag/AgCl reference electrode and a Pt auxiliary electrode. The exposed electrode surface area was 1.0 cm^2 and scan rate was 50 mV/s.

3. Results and Discussion

Table I summarizes the KPM results, where the surface potential is given by

$$V_s = \frac{\mu N_s}{\varepsilon_0 \varepsilon} S_1 . \qquad (1)$$

The effective dipole moment (μ/ε) of SAM and lipid are 0.3D and 0.75D, respectively.

Table I KPM results

	a. SAM (vs Au)	b. Lipid (vs Au)	c. Lipid (vs SAM)	d. HBM (vs Au)
Calculation	650 mV	430 mV	-430 mV	120 mV
Result	480 mV	630 mV	105 mV	620 mV
Ref. 11, 12	600 mV	400 mV	None	None

(The "vs" in Table represents the reference electrode.)

The morphology and related physical properties were examined by AFM and KFM (or KPM). The AFM and KFM images of the p-SAM in air revealed that the pattern with a distance of about 900 nm and height of about 2 nm were successfully prepared. Here the value of this height corresponds to the thickness of HXDT-monolayer (Fig.2 (a)). The surface potential of the p-SAM is about 120 mV with reference to the Au surface (Fig.2 (b)). The surface potential of SAM (vs Au) is about 450 mV (Table 1), similar to the result by Ulman et.al [11], but this value is a little difference from that obtained by KFM. Note that, these two measurements principles are different in their methods and they are as follows;

For KPM:

$$I(t) = \frac{dQ(t)}{dt} \cong -(V_{ex} - V_s) C_0 \omega \frac{l_v}{l_0} \cos \omega t \qquad (2)$$

For KFM:

$$F = -\frac{1}{2}\frac{\partial C}{\partial z}\{(V_s + V_{DC})^2 + (V_s + V_{DC})V_{AC}e^{i\omega t} \quad (3)$$
$$+V_{AC}{}^2 e^{i2\omega t}\}$$

Furthermore, the physical property of p-SAM was nearly the same as that made by immersing method [13], and the contact angle was also nearly the same each other.

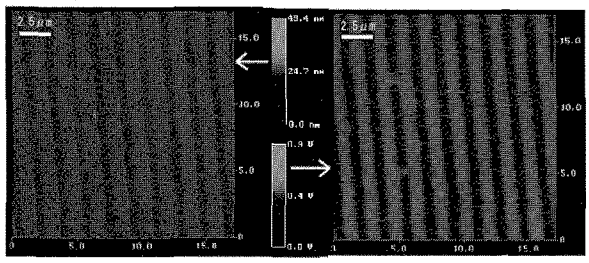

(a) (b)

Figure 2 AFM (a) and KFM (b) images of p-SAM

Fig. 3 (a) and (b) shows AFM and KFM images of HBM in air, respectively. In Fig. 3 (a), lipid thickness is about 8 nm. This thickness corresponded to lipid triple layer. This result was different from that we expected, but the orientation of the lipid molecule was as illustrated in Fig.1 (a). From molecular structure, polar ester group of molecule and head group are main origin of dipoles. The latter one lies parallel to the planer monolayer, hence the ester group is main origin of surface potential. The C=O carbonyl points downward in Fig. 4. If lipid monolayer is formed on the SAM, surface potential should be negative. In Fig. 3 (b), KFM image shows that surface potential of lipid monolayer was about –350 mV revealed that lipid is triple layer, where the dipole points downwards, supporting our calculation in Table I (c).

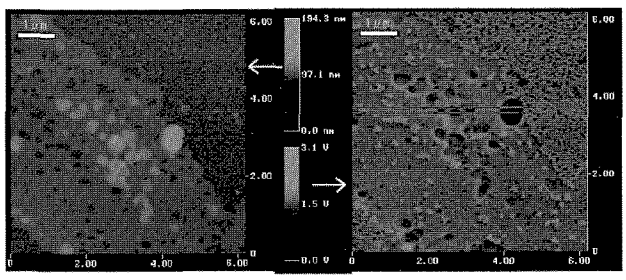

(a) (b)

Figure 3 AFM (a) and KFM (b) images of lipid monolayer on SAM (HBM)

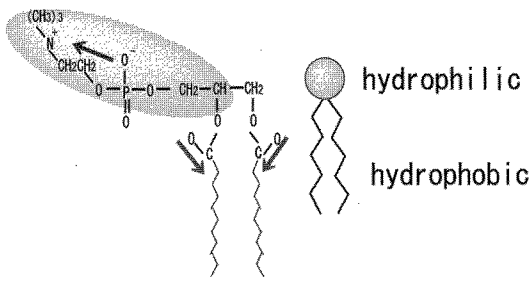

Figure 4 Lipid dipole

Figs. 5 (a), (b) and (c) show the tapping-mode AFM height, phase and KFM images of DPPC lipid layer on p-SAM in air, respectively. The phase image and KFM image (Fig. 5 (b) and (c)) reveal contrast along the lined pattern, whereas the height image (Fig. 5 (a)) does not show any contrast. Note that the contact-mode AFM revealed the thickness of about 5 nm corresponds to the thickness of lipid planar bilayer. As described in § 2.4, the phase image is reflects the visco-elasticity of surface. SAM is chemically adsorbed on Au surface, while lipid is softly deposited. The visco-elasticity of SAM is lower than that of lipid. In Fig. 5 (b), circle area is assigned to lipid monolayer (SAM) area and star area is lipid bilayer area. From Fig. 5(b) with Fig. 5 (c), surface potential of lipid bilayer area is higher than that of lipid monolayer area. In the bilayer area, the magnitude of lipid dipole is the same but direction is opposite. In the monolayer area, lipid dipole and SAM dipole is opposite and magnitude is different. As listed in Table I, surface potential of SAM is bigger than that of lipid. On the other hand, from Fig.2 (b) and Fig. 3 (b), surface potential of SAM is smaller than that of lipid. Here surface potential of Fig. 2 and Fig. 3 was estimated with reference to Au surface. The surface potential of lipid monolayer on the SAM was lower than that of Au surface. This conclusion was supported in Fig. 5 (c). Surface potential of lipid monolayer on the SAM is about –250 mV with referenced to Au surface (lipid bilayer surface). And this value nearly corresponded to the difference between Fig. 2 (about 120 mV) and Fig. 3 (about –350mV). These results show that the lipid layer overcoats the p-SAM well. In other words, an artificial bilayer was prepared on the surface without SAM and single lipid layer on the surface of SAM, in a manner as illustrated in Fig.1 (b). Note that in Fig. 5 (a), artifacts were also observed, owing to condensation of lipid bilayer.

Finally, Fig.6 shows the result of CV, using a solution of 1 M KCl included 1 mM $K_3Fe(CN)_6$. By the deposition of SAM or p-SAM, the peak current observed to Au decreased. In more detail, the region coated with SAM blocked the redox reaction, and the peak CV current of the p-SAM decreased to the half of that of pure Au. The peak current of CV of HBM and p-HBM (dot line) decreased more. HBM result indicates that the HBM works as a good electrical insulating barrier, and effectively blocks the electrochemical reaction. In particular, p-HBM result suggests that the deposition of lipids went well over the entire region of the substrate with p-SAM, and the redox-reaction was blocked by the deposition, though we need to improve the film quality.

4. Summary

Micro-patterned composite membranes of fluid lipid bilayer and stable lipid monolayer were prepared using a μCP method. The AFM and KFM observation were conducted using height, phase imaging modes and surface potential imaging, respectively. The result of height imaging showed that the flat surface was made by the μCP method. Furthermore, the result of phase imaging and KFM imaging revealed the image of the micro-pattern. These results show that an artificial bilayer was successfully prepared on the surface without

SAM and lipid monolayer on the surface with SAM. And KFM results revealed that the dipole of lipid monolayer on the surface of SAM points downwards and that of lipid bilayer on the surface without SAM is canceled.

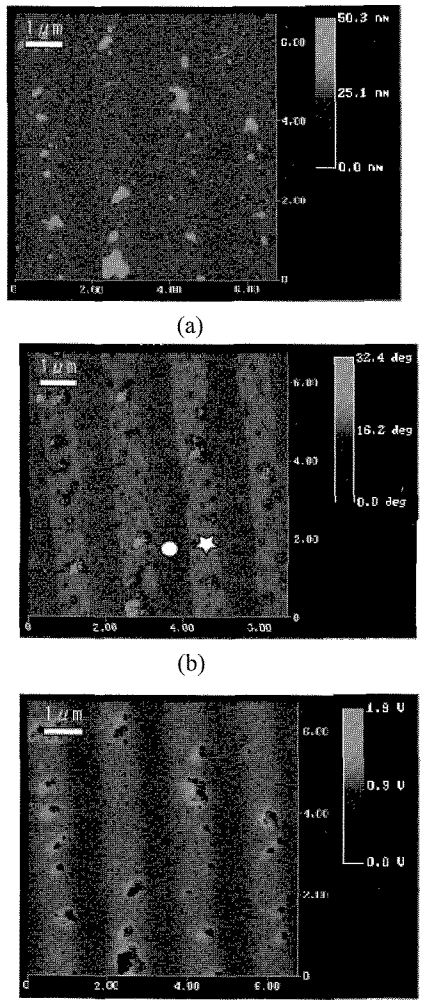

Figure 5 AFM (a) height mode, (b) phase mode and (c) KFM images of lipid layer on p-SAM (p-HBM).

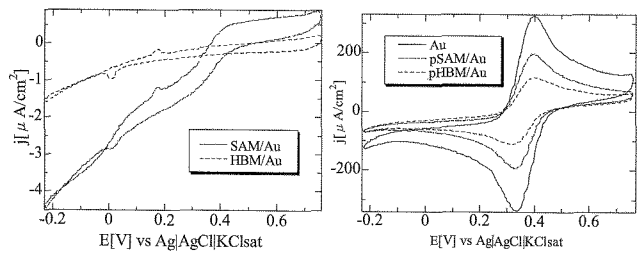

Figure 6 Cyclic voltammograms: (a) HBM, (b) p-HBM

Reference

[1] S. J. Singer and G. L. Nicolson, *Acta Europ. J. Cell Biol.*, **175**, 720-731 (1972).
[2] H. T. Tien and A. Ottova, *IEEE Trans. Dielectrics and Electr. Insul.*, **10,** 717-727 (2003).
[3] Y. Nishimura, R. Wagner, T. Manaka and M. Iwamoto, *Thin Solid Films,* **499,** 40-43 (2006).
[4] Y. Nishimura, T. Manaka and M. Iwamoto, *Thin Solid Films,* submit
[5] R. C. MacDonald, R. I. MacDonald, D. M. Menco, K. Takeshita, N. K. Subbarao and Lan-rong Hu, *Biochim. Biophys. Act.,* **1061**, 297-303 (1991).
[6] E. Kalb, S. Frey and L. K. Tamm, *Biochim. Biophys. Acta.,* **1103**, 307-316 (1992).
[7] A. L. Plant, *Langmuir,* **9**, 2764-2767 (1993).
[8] R. Lipowsky and U. Seifert, *Mol. Cryst. Liq. Cryst.,* **202**, 17-25 (1991).
[9] A. Kumar and G. M. Whitesides, *Appl. Phys. Lett.*, **63,** 2002-2004 (1993).
[10] Y. Xia, J. Tien, D. Qin and G. M. Whitesides, *Langmuir,* **12,** 4033-4038 (1996).
[11] S. D. Evans and A. Ulman *Chem. Phys. Lett.,* **170,** 462-466 (1990).
[12] W. M. Heckl, H. Baumgärtner and H. Möhwald, *Thin Solid Films,* **173,** 269-278 (1989).
[13] R. G. Nuzzo, F. A. Fusco and D. L. Allara, *J. Am. Chem. Soc.,* **109,** 2358-2368 (1987),

(Received December 5, 2007;Accepted Febrary 15, 2008)